



## Comparison Between Th-U-REE Mineralizations of Rhyolite Volcanics and Its Intrusive Equivalent: A Case Study at Structurally Related Mineralizations at Um Safi and W.Ras Abda Areas, Eastern Desert, Egypt



Anton G. Waheeb, Hassan I. El Sundoly, Mohamed M. Hassan, Hicham M. Abdel Hamid and Siddiq H. Siddiq

*Nuclear Materials Authority, Cairo, Egypt*

ONE of the most favourable host rocks for REE metals in the Central Eastern Desert of Egypt is the Um Safi rhyolitic volcanics, which are thought to have a high potential source of REE metals associated with mostly thorium radioactive materials. Whereas, W. Ras Abda alkali feldspar high-K calc-alkaline perthitic granite is considered a high potential source for radioactive minerals in the Northern Eastern Desert of Egypt.

The presence of REEs, Th, and U mineralizations in both rhyolitic volcanic rocks at Um Safi and at intrusive granitic rocks of W. Ras Abda areas are greatly controlled by internal tectonics that are related to the same extensional phase of deformation (WNW-ESE to E-W). The radioactivity in Um Safi area is higher than in W. Ras Abda but the W. Ras Abda area is richer in uranium minerals than Um Safi area. Uranophane, Uranothorite, and thorite are detected at Wadi Ras Abda area; while thorite is identified at Um Safi area.

The resolved shear stress structural analysis indicates the direction of shear stress ( $\tau$ ) on Um Safi rhyolitic volcanics as N-S direction, where it is slightly shifted to NNE-SSW and NE-SW at W. Ras Abda granitic mineralized fault zones.

**Keywords:** Paleostress Analysis, Shear Direction, REE Metals and Thorium, Mineralized Tectonic Faults, Um Safi and W.Ras Abda Areas.

### 1. Introduction

The regions under investigation are found in the Eastern Desert of Egypt. Safaga is the closest town to the W. Ras Abda region. However, the town closest to the Um Safi area is Marsa Alam. Latitudes 25°17'33" to 25°19'48" N and longitudes 34°07'02" to 34°08'54" E define the boundaries of the Um Safi area. Latitudes 26° 43' 22" to 26° 43' 30" N and longitudes 33° 45' 35" to 33° 45' 52" E define the boundaries of the W. Ras Abda granite (Fig.1).

The youngest and most felsic and silicic elements of igneous rocks include large amounts of uranium and thorium. A type of felsic igneous rock containing high concentrations of the two elements is metaluminous high-K alkaline to calcalkaline rocks (Cuney, 2009). Three distinct kinds of felsic igneous rocks have been recognized as the source of uranium worldwide (France: Scaillet et al., 1996; Namibia: Nex et al., 2001; Germany: Dill et al., 2010; China: Zhao et al., 2011; Ukraine: Cuney et al., 2012). Also, felsic volcanic rocks are frequently found to be enriched in rare metals, including radioactive elements such as Th and U (Castor and Henry 2000; Nash 2010; Cuney and Kyser 2015).

W. Ras Abda mineralized granitic rocks are structurally controlled and the hydrothermal vein-type radioactive mineralizations that are associated with the granitic rocks are predominantly tectonic faults controlled (Cuney, 2003). IAEA (2013) classified volcanic radioactive mineralization as structure-bound or strata-bound sub-types. Radioactive mineralizations associated with Um Safi volcanics are mainly controlled by tectonic faults, so it is a structurally bounded sub-type.

Northern Eastern Desert (NED) of Egypt is dominated by felsic magmatism and is considered a source of radioactive minerals such as W. Ras Abda's alkali feldspar high-K calc-alkaline perthitic granite (Abdel Hamid et al 2018). (NED) is characterized by An important change in tectonic style from compressional to extensional that occurred 620–600 million years ago, and the magmatic activity that identified the final phase of the cratonization process by which the Pan African orogeny formed in the last stage of the shield evolution (Stern et al., 1984; Bentor, 1985; Kroner et al., 1987; Stern, 1994; Genna et al., 2002; Meert,2003).

\*Corresponding author e-mail: anton\_oon@yahoo.com

Received: 07/11/2024; Accepted: 25/11/2024

DOI: 10.21608/egjg.2024.324949.1092

©2025 National Information and Documentation Center (NIDOC)

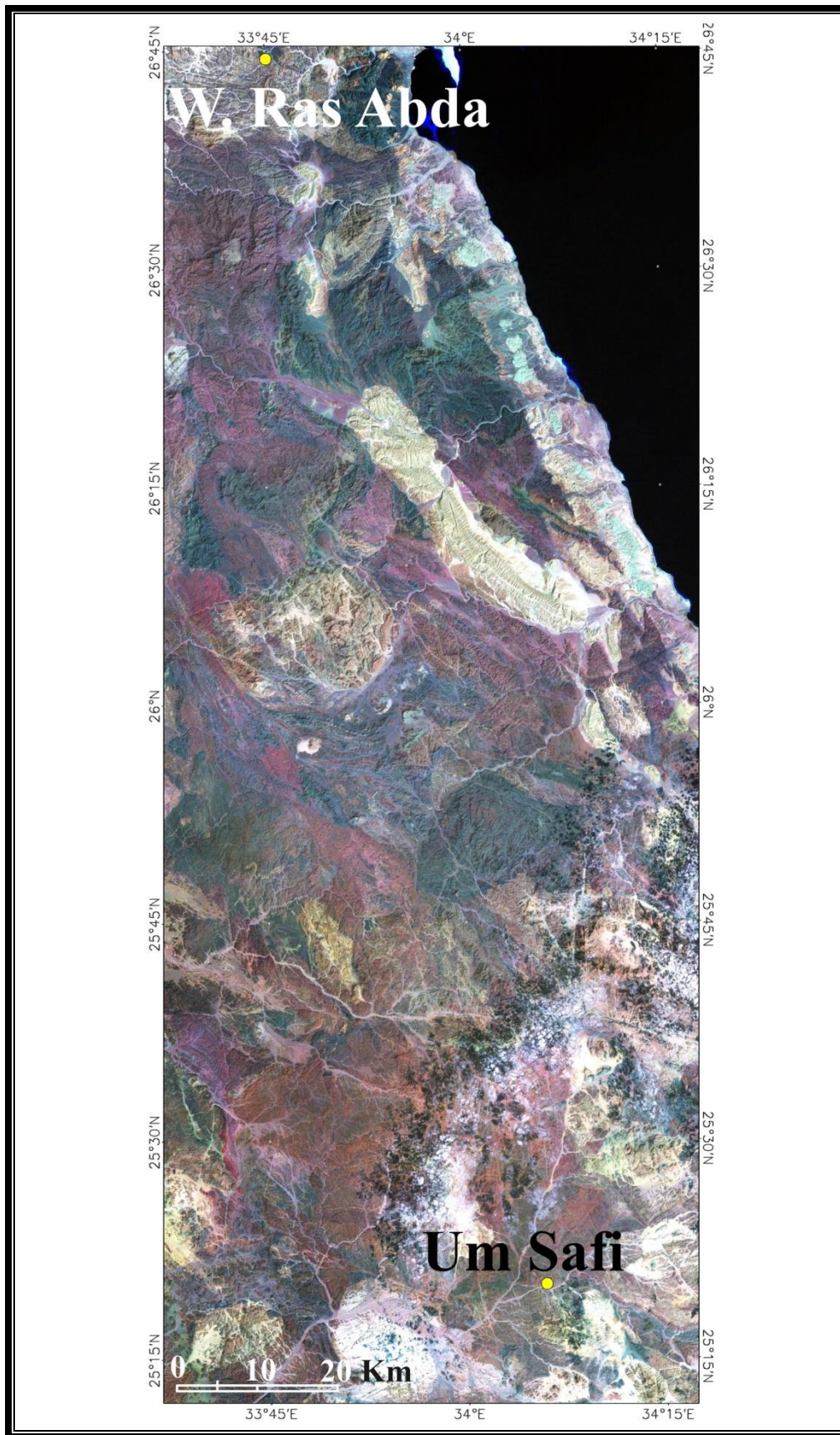


**Fig. 1.** Land sat image for Um Safi and W. Ras Abda areas.

W. Ras Abda granite is distinguished by having a higher concentration of thorium than uranium, with an average of 14.3 ppm for eU and 37.6 ppm for eTh. (Omran, 2005, Omran, 2015 and El Hadary et al, 2013) Suggesting a fertile-Th source.

Um Safi rhyolitic volcanics at the Central Eastern Desert of Egypt are thought to have a high potential source of REE metals associated with mostly thorium radioactive minerals. Um Safi area has thorium content more than uranium where an average of eU is 33 ppm while that of eTh is 73 ppm as we note that the rhyolitic volcanics at Um Safi are 1.5 or 2 times higher and richer in radioactive elements content than their intrusive granitic equivalents at W. Ras Abda and this is also mentioned by Klepper and Wyand 1956.

In this paper, the shear stress, paleostress analysis, and mineralogical investigation of structurally controlled radioactive occurrences at W. Ras Abda granite and Um Safi rhyolitic volcanics were carried out to compare between the shear stress required initiating slip, the extensional phase that causes the localization of radioactive minerals and minerals constitute on these areas.

## 2. Structure and radioactivity

Mineralization in Um Safi area is confined to the rhyolite and the mineralized domains of the rhyolite are intensively altered and fractured. The mineralized zones of the rhyolite are rich in REEs, Th, and poor in U as radiometrical and mineralogical analysis indicated. The radioactive sheared zones at Um Safi area is trending in the N-S direction with a dipping of  $88^\circ$  to E (Fig.2). The radioactivity in Um Safi area is high and ranges from 300 to 12000 ppm.

The radioactive mineralization at Ras Abda granite is also structurally controlled; the radioactive sheared zones at the Ras Abda area are trending in  $N40^\circ E$ , and the dip ranges between  $82^\circ$  and  $86^\circ$  to SE along a strike-slip fault and a normal fault, respectively (Fig. 3). Also, the radioactivity in the Ras Abda area is high and ranges from 500 to 9500 ppm. Uranium, thorium, and black rare metal minerals are identified by the necked eye along shear zones in Ras Abda granite (Fig. 4).

## 3. Materials and Methods

Laboratory and field activities, including examinations of minerals. Field measurements of radioactivity are performed using the gamma-ray scintillometer, model RS-320. With this device,



**Fig. 2.** mineralized fault zone of a major normal fault trending NS with dips of about  $88^\circ$  to E. Looking N, Um Safi area.



**Fig. 3.** Mineralized normal fault striking  $N40^\circ E$  and the dip is  $86^\circ$  to SE, W. Ras Abda area. Looking E.



**Fig. 4.** (REE) metals associated with thorium and uranium minerals along sinistral strike lip fault trending  $N40^\circ E$  with dipping  $82^\circ$  SE, W. Ras Abda area. Looking E.

the radioactivity of the rocks is expressed in parts per million (ppm).

Field photographs are captured in different locations to showcase the various characteristics of the areas under investigation. A graphical technique (Lisle, 1998) was used to predict the direction of the highest resolved shear stress on a fault plane for the mineralized shear zones in the granites of W. Ras Abda and the rhyolite of Um Safi. Knowing the orientations of the three main stress axes as well as the stress ratio is necessary for using this graphical method. These data are produced using the Improved Right Dihedron paleostress fault analysis method (Delvaux and Sperner 2003) for shear zone fault planes.

A few samples were selected from the areas under study because of their high level of radioactivity for the separation of heavy minerals, following crushing, grinding, and sieving, the samples were subjected to heavy mineral separation using bromoform (sp. gr. = 2.85 gm/cm<sup>3</sup>). They were then cleaned, and dried. Pure mineral grains were hand-picked from the resulting heavy fractions to the heavy minerals. Using a backscatter detector (BSE), the Environmental Scanning Electron Microscope (ESEM) analyzed the separated heavy minerals. This device includes a Philips XL 30 energy-dispersive X-ray (EDAX) unit. The studies were conducted at Nuclear Materials Authority (NMA), Egypt using analytical settings that included an accelerating voltage of 30 kV.

#### 4. Results

##### 4.1 Paleostress analysis

Finding the stress tensor components  $\sigma_1$ ,  $\sigma_2$ , and  $\sigma_3$  as well as the ratio of the principal stress difference  $\Phi$  or  $R$   $\{\Phi = (\sigma_2 - \sigma_3) / (\sigma_1 - \sigma_3)\}$  are among the main aims of the paleostress study (Etchecopar 1984). The development of the paleostress analysis technique using microtectonic data to determine the causative stress tensors was aided by many studies, including Orife and Lisle (2003), Liesa and Lisle (2004), Shan *et al.* (2004 and 2006), Sato and Yamaji (2006), Otsubo *et al.* (2006), and Zalohar and Vrabc (2007). A paleostress analysis of the radioactive faults in both locations of the investigation was carried out.

At Um Safi area,  $\sigma_1$  plunges 80° on bearing 28°,  $\sigma_2$  plunges 9° on bearing 186°,  $\sigma_3$  plunges 4° on bearing 277° and stress ratio  $\Phi$  is 1 (Fig.5); while at W.Ras Abda area,  $\sigma_1$  plunges 51° on bearing 283°,  $\sigma_2$  plunges 13° on bearing 29°,  $\sigma_3$  plunges 36° on bearing 129° and stress ratio  $\Phi$  is 0 for N40°E

normal fault with a dipping of 86° to SE (Fig.6) and for the mineralized N40°E sinistral strike-slip fault which dips 82° to SE,  $\sigma_1$  plunges 17° on bearing 335°,  $\sigma_2$  plunges 73° on bearing 191°,  $\sigma_3$  plunges 4° on bearing 86° and stress ratio  $\Phi$  is 0.5 (Fig. 7).

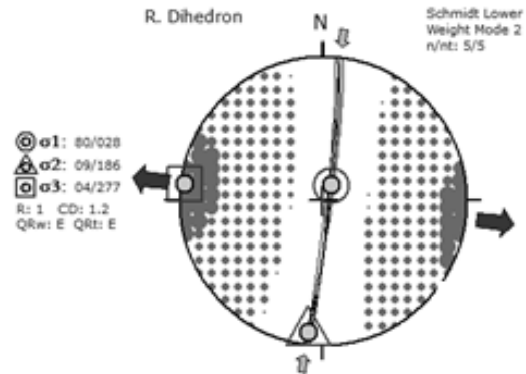


Fig. 5. Three principal stress axes for mineralized normal fault at Um Safi area.

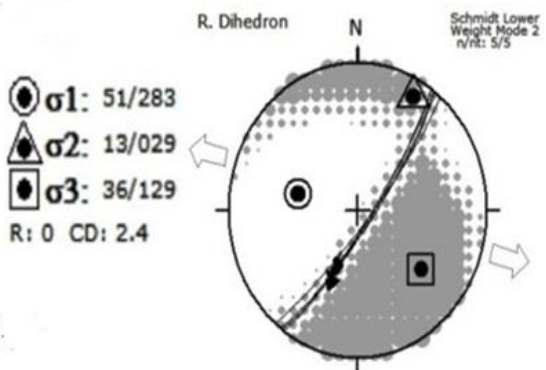


Fig. 6. Three principal stress axes for mineralized normal fault at W. Ras Abda area.

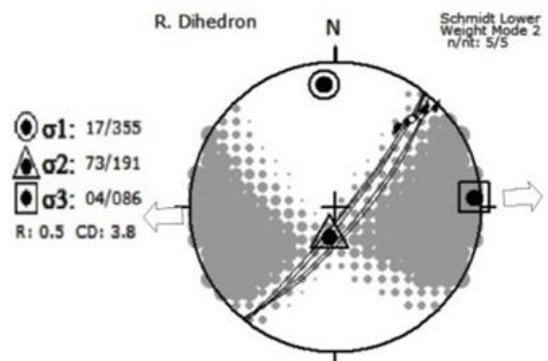


Fig. 7. Three principal stress axes for mineralized strike-slip fault at W. Ras Abda area.

The structural analysis shows that the WNW-ESE to E-W extensional phase of deformation is the main phase of deformation that controls the distribution of mineralizations at both Um Safi and W. Ras Abda areas.

**4.2 Maximum resolved shear stress ( $\tau$ )**

The Lisle (1998) method can be used to graphically establish the fault plane's perpendicular direction, which yields the resolved shear stress ( $\tau$ ). Many structural geologists have tackled the problem of determining the resolved shear stress ( $\tau$ ) on a given planar surface (e.g., Johnson and Mellor, 1973; Lisle, 1989, 1998; Means, 1989; DePaor, 1990; Ragan, 1990; Fry, 1992; Fleischmann, 1992; Ritz, 1994). Even though the shear on the surface can be easily calculated statistically, determining it directly in a pictorial format might be challenging. In their unique ways, all of the current techniques were developed to directly search for the direction of the resolved shear stress ( $\tau$ ) on the surface.

The orientations of the primary stress axes and the ratio of the principle stress differences can be used to determine the resolved shear stress( $\tau$ ), as shown by a new graphical approach (Lisle method 1998) that follows below. Along the mineralized fault zones where radioactive minerals are found in both the Um Safi and W. Ras Abda areas, resolved shear stress ( $\tau$ ) is determined.

At Um Safi area, the resolved shear stress ( $\tau$ ) plunges 68° on bearing 181°( N-S )for the mineralized fault zone of a major normal fault trending NS with dips of about 88° to E. (Fig.8).

At W. Ras Abda area, the resolved shear stress ( $\tau$ ) plunges 68° on bearing 208° (NNE-SSW)for N40°E normal fault with dipping 86° to SE (Fig.9)and the resolved shear stress ( $\tau$ ) plunges 2° on bearing 40°(NE-SW)for the mineralized N40°E sinistral strike-slip fault with dipping 82° to SE (Fig. 10).

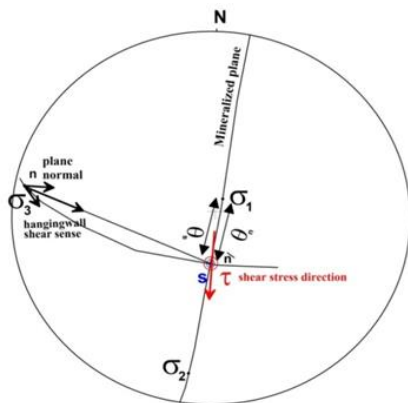


**Fig. 8. Graphical method to determine the direction of shear( $\tau$ )on Um Safi rhyolitic mineralized fault plane.**

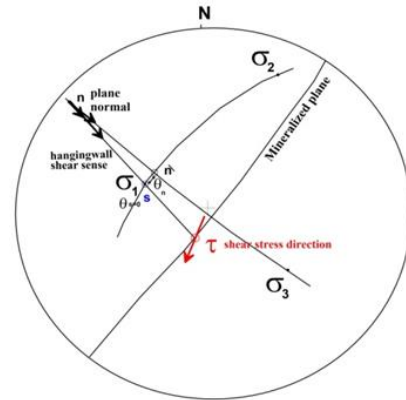


**Fig. 9. Graphical method to determine the direction of shear( $\tau$ )on granitic mineralized N40°E normal fault with dipping 86° to SE at W.Ras Abda area.**

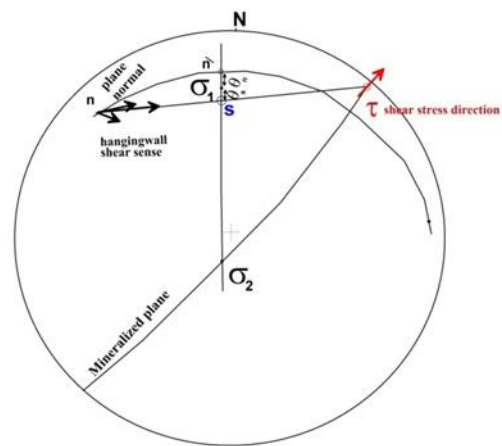


**Fig. 10. Graphical method to determine the direction of shear( $\tau$ )on granitic mineralized N40°E sinistral strike-slip fault with dipping 82° to SE at W.Ras Abda area.**

The above-mentioned structural analysis indicates that the direction of maximum resolved shear stress ( $\tau$ )(the direction of stress required initiating slip at Um Safi rhyolitic mineralized fault plane)is directed N-S; while the direction of maximum resolved shear stress ( $\tau$ )at W. Ras Abda granitic radioactive mineralized fault zones is directed NNE-SSW to NE-SW.

**4.3 Mineralogy**

The rare metal (Y-Yb)-bearing mineral in the rhyolite of Um Safi area include xenotime (Fig.11) and unidentified (Th-As-Y)-rich materials (Fig.12c-d), thorite are also identified by (ESEM)(Fig .12a-b). Semi-quantitative evaluation analysis of thorite confirmed the presence of Th = 72.5% and Si =19.6% associated with minor content of Fe = 4.4 % and Al= 3.6 % (table.1); while, Uranothorite, thorite, and uranophane are identified at Wadi Ras Abda area, as well as; (REE) bearing fergusonite mineral as identified by (ESEM) (Waheeb and El

Sundoly 2020). The existence of Th = 61.17% and Si = 17.68%, along with a low content of U = 8.65%, was confirmed by semi-quantitative evaluation analysis of thorite (Fig. 13a), while Th = 46.09%, U = 25.25%, Si = 20.17%, and Ca = 1.7% were found in uranothorite (Fig. 13b). There are very small quantities of uranophane, a hydrated uranyl silicate. Fig. 13c shows fibrous radial crystals radiating from the center, and the REE(Y-Nb)-bearing fergusonite mineral is also identified. BSE image and EDAX analysis of Fergusonite are displayed in (Fig. 13d).

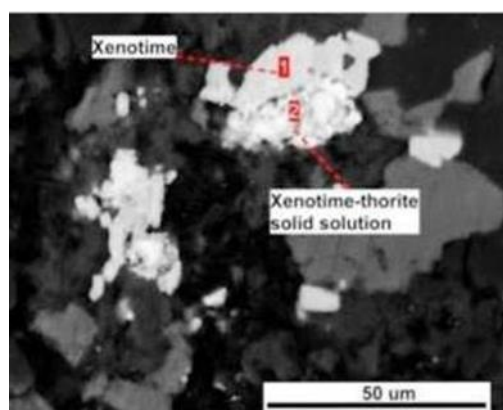


Fig. 11. BSE image showing Xenotime forming a solid solution with thorite on its rim. Numbers refer to semi-quantitative spot analyses of the minerals in Table 1.

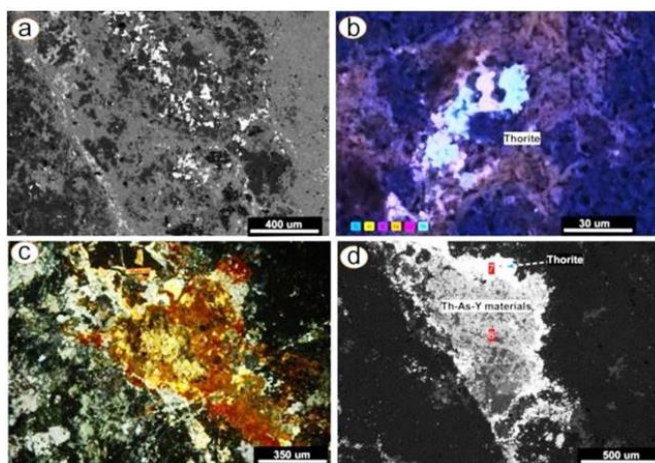


Fig. 12. (a) BSE image shows the abundance of thorite in the rhyolite, which is intimately associated with iron oxides. (b) Color SEM of various elements in thorite. (c- d) Thorite occurs on the rim of unidentified Th-As-Y-rich materials. Numbers refer to semi-quantitative spot analyses of the minerals in Table 1.

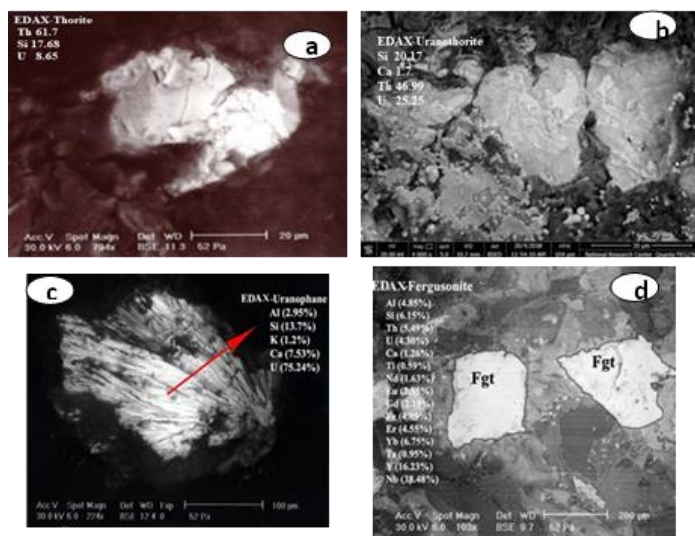


Fig. 13. BSE image and EDAX showing (a) thorite, (b) uranothorite, (c) uranophane, and (d) fergusonite at W. Ras Abda area.

Table 1. Semi-quantitative spot analyses of the minerals and materials associated with rhyolite rocks using SEM.

Element wt.%	1- Xenotime	2- Xenotime-thorite solid solutions	7- Thorite	8-Th-As-Y rich materials
Al	2.2	5.8	3.6	3.0
Si	2.8	22.9	19.6	17.0
K	1.3			
Fe			4.4	14.2
Th		40.5	72.5	15.3
Ca	3.7	7.9		5.3
Na				0.5
As				12.2
Y	50.0	9.0		30.9
Yb	15.9			
P	24.1	10.9		1.6

## 5. Discussion

Mineralizations in Um Safi area are xenotime and thorite and confined to the rhyolite and are detected along radioactive sheared zones that trend in the N-S direction with dipping  $88^\circ$  to E. But at W. Ras Abda area the radioactive sheared zones are trending in  $N40^\circ E$ , and the dip ranges between  $82^\circ$  and  $86^\circ$  to SE along a strike-slip fault and a normal fault, respectively, and is confined to the granites.

The two trends N-S and NE-SW trends with extremely steep dip angles are the primary

structural fabric elements that regulate the distribution and localization of radioactive mineralization in the areas under investigation. These two trends are related to the same phase of deformation which is the WNW-ESE to E-W extensional phase of deformation as indicated by paleostress analysis. The radioactivity in Um Safi area is higher than in W. Ras Abda but W. Ras Abda area is richer at uranium minerals than Um Safi area.

The direction of resolved shear stress( $\tau$ ) for the mineralized fault zones; which are considered the most important zones along which the radioactive minerals are emplaced in the investigated areas indicate that it is directed NNE-SSW to NE-SW at W. Ras Abda area, where, it plunges 60° on bearing 213° (NNE-SSW) and plunges 21° on bearing 42°(NE-SW); while the direction of resolved shear stress ( $\tau$ ) on Um Safi area differs and it is directed N-S; as it plunges 43° on bearing 181°( N-S).

## 6. Conclusion

The main host rock for mineralizations at the Northern Eastern Desert of Egypt is granite (intrusive), whereas the main host rock for mineralizations at the Central Eastern Desert of Egypt is volcanic rocks (trachyte and rhyolite) in association with granite. The volcanic rocks are 1.5 or 2 times higher and richer in radioactive element content than their intrusive granitic equivalents.

The presence of REEs, Th, and U mineralizations in both intrusive granitic rocks of W. Ras Abda and rhyolitic volcanic rocks at Um Safi areas are greatly controlled by internal tectonics which makes these occurrences more suitable for radioactive mineralization localization. The rare metal minerals in the rhyolites of Um Safi area are xenotime and unidentified Th-As-Y-rich materials while fergusonite is at Wadi Ras Abda, thorite is also identified in Um Safi area but Uranothorite, thorite, and uranophane are determined at Wadi Ras Abda area.

The main phase of deformation that controls the distribution of mineralizations at both Um Safi and W. Ras Abda areas is the same (The WNW-ESE to E-W extensional phase of deformation). The resolved shear stress ( $\tau$ ) on Um Safi rhyolitic volcanics is directed N-S where; it is slightly shifted to NNE-SSW and NE-SW at W. Ras Abda granitic mineralized fault zones.

**Conflicts of Interest:** The author declares no conflict of interest.

**Acknowledgements:** The authors would like to thank Prof. D. M. El Kholy of the Nuclear Materials Authority for his many insightful conversations as well as his critical evaluations and recommendations, which greatly enhanced the manuscript's quality. We are grateful to Prof. Jehan and the Nuclear Materials Authority's Scanning Electron Microscope Lab team for their invaluable assistance in conducting the electron microscope scan analysis.

## 7. References

- Abdel Hamid, A. A., El Sundoly, H. I., and Abu Steet, A. A.(2018) . Hydrothermal alteration and evolution of Zr-Th-U-REE mineralization in the microgranite of Wadi Ras Abda, North Eastern Desert, Egypt. *Arabian Journal of Geosciences*. <https://doi.org/10.1007/s12517-018-3623-2>.
- Bentor, Y.K.(1985). The crustal evolution of the Arabo-Nubian Massif with special reference to the Sinai Peninsula. *Precambrian Research* **28**: 1–74.
- Castor, S. B. and Henry, C.D. (2000). Geology, geochemistry, and origin of volcanic rock hosted uranium deposits in northwestern Nevada and southern Oregon, US. *Ore Geol. Rev* **16**: 1-40.
- Cuney, M. ( 2003). Uranium potential of Eastern Desert granite, Egypt. *Unpublished Internal Report, Nuclear Materials Authority, Cairo, Egypt*.
- Cuney, M.( 2009). The extreme diversity of uranium deposits. *Mineralium Deposita* **44**, 3–9.
- Cuney, M., and Kyser, T. K.( 2015). Geology and geochemistry of uranium and thorium deposits. *Miner Assoc Can Short Course* 46:345.
- Cuney, M., Emetz, A., Mercadier, J., Mykchaylov, V., Shunko, V. and Anatoliy Yuslenko, A. (2012). Uranium deposits associated with Na-metasomatism from central Ukraine: A review of some of the major deposits and genetic constraints. *Ore Geol. Rev.* **44**: 82-106.
- Dahlkamp, F.J.(2009). Uranium Deposits of the World: Asia. *Springer*, p. 493.
- Delvaux, D. and Sperner, B. (2003). New aspects of tectonic stress inversion with reference to the TENSOR program. *Geological Society, London, Special Publications*, v. **212**, pp. 75–100.
- Dill, H. G., A. Gerdes, A. Weber, B. (2010). Age and mineralogy of supergene uranium minerals-Tools to unravel geomorphological and palaeohydrological processes in granitic terrains (*Bohemian Massif, SE Germany*). *Geomorphology* **117**: 44–65.
- EL Hadary A., El Azab A., and Omran A.A. (2013). Contributions to the geology and mineralogy of Wadi Ras Abda area, North Eastern Desert, Egypt. *Nuclear Sciences Scientific Journal*. **V. 2**.
- El-Kammar, A.M., Salman, A.E., Shalaby, M.H., Mahdy, A.I. (2001). Geochemical and genetical constraints on

- rare metals mineralizations at the central Eastern Desert of Egypt. *Chemical Journal* **35**, pp.117–135.
- El Sundoly, H. I. and Waheeb, A. G.( 2015).A New Genetic Model, For The Localization of Uranium Minerals At The Northern part of Gabal Gattar, North Eastern Desert, Egypt. *3rd Symposium of the Geol. Res. in the Tethys Realm, Cairo Univ.* 21-39.
- Etchecopar, A. (1984). Etude des états de contraintes en tectonique cassante et simulation de déformations plastiques (*approche mathématique*). *These Doctorat-es-Sciences, Univ. Sciences, et Techniques Languedoc, Montpellier*, 270p.
- Fry, N. (1992). Direction of shear. *J. Struct. Geol.*, **V.14**, pp.253–255.
- Genna, A., Nehlig, P., Le Goff, E., Guerrot, C. and Shanti, M.( 2002). Proterozoic tectonism of the Arabian Shield. *Precambrian Research* **117**: 21–40.
- IAEA (2013). Uranium deposit classification. *Vienna, Austria*
- Klepper,M.R., and Wyant,D.G.( 1956). Uranium provinces : in page,L.R.,Stocking,H.E., and Smith H.B.,eds., Contribution to the geology of uranium and thorium by the US Geological Survey and Atomic Energy Commission for the United Nations *Int.Conf. on peaceful uses of atomic energy, Geneva, Switzerland,1955, U, S, Geological Survey Professional paper* **300**,p,17-26.
- Kröner, A., Greiling, R., Reischmann, T., Hussein, I.M., Stern, R.J., Durr, S., Krugger, J. and Zimmer, M. (1987). Pan-African crustal evolution in the Nubian segment of north-eastern Africa. In: Kröner, A. (Ed.), Proterozoic Lithospheric Evolution Am. *Geophys. Union Geodynamic Series* **15**, p. 235–257.
- Liesa, C.L. and Lisle, R.J. (2004). Reliability of methods to separate stress tensors from heterogeneous fault-slip data. *J. of Struct. Geol.* **26**, 559-572.
- Lisle, R.J. (1989). A simple construction for shear stress. *J. Struct. Geol.*, **V. 11**, pp.493–495.
- Lisle, R.J. (1998). simple graphical constructions for the direction of shear. *J. Struct. Geol.*, **V.20, No.7**, pp. 969 - 973.
- Means, W.D.( 1989). A construction for shear stress on a generally-oriented plane. *Journal of Structural Geology* **11**, 625–627
- Meert, J.G. (2003). A synopsis of events related to the assembly of eastern Gondwana. *Tectonophysics* **362**: 1–40.
- Nash, J. T. (2010). Volcanogenic uranium deposits-Geology, geochemical processes and criteria for resource assessment: *US Geological Survey Open File Report 2010-1001*, p99.
- Nex, P. A., Kinnaird, J. A., Oliver, G. J. (2001). Petrology, geochemistry and uranium mineralisation of post-collisional magmatism around Goanikontes, southern Central Zone, Damaran Orogen, Namibia. *Journal of African Earth Sciences* **33**: 481–502.
- Omran A. A. (2005). Geological, petrochemical studies and potentiality of uranium-thorium occurrences in Gabal Um Taghir El-Tahtani area with emphasis on the granitic rocks, Central Eastern Desert, Egypt. *Ph.D. thesis, Ain Shams Univ., Cairo, Egypt*. 189 p
- Omran,A, A. (2015). Geology, mineralogy and radioelements potentiality of microgranite dykes to the south of wadi Abu Hadedia area, Northern Eastern Desert, Egypt. *Al-Azhar Bull Sci* **26**:67–89
- Orife, T. and Lisle, R.J. (2003). Numerical processing of paleostress results. *J. Struct. Geol.*, **v. 25**, pp. 949-957.
- Otsubo, M.; Sato, K. and Yamaji, A.( 2006). Computerized identification of stress tensors determined from heterogeneous fault-slip data by combining the multiple inverse method and k-means clustering. *J. Struct. Geol.*, **v. 28**, pp. 991-997.
- Rashwan, A. A., Shalaby, M. H., Roz, M. E., Wetait M. A., and Abdel Hamid A. A. (2013): Alkalic-metasomatism and redistribution of U, Th and REE in the hydrothermally altered granite of Gabal Abu Harba, North Eastern Desert, Egypt. *Nuclear Science Scientific journal*, **Vol. 2**, p23-37.
- Sato, K., and Yamaji, A. (2006). Embedding stress difference in parameter space for stress tensor inversion. *J. Struct. Geol.*, **v. 28**, pp. 957-971.
- Scaillet, S., Cuney, M., Le Carlier De Veslud, C., Cheilletz, A., and Royer, J. J., (1996). Cooling pattern and mineralization history of the Saint Sylvestre and western Marche leucogranite pluton, French Massif Central: II. Thermal modeling and implications for the mechanisms of uranium mineralization. *Geochimica et Cosmochimica, Acta* **60**: 4673-4688.
- Shan, Y.; Lin, G. and Li, Z. (2004). A stress inversion procedure for automatic recognition of polyphase fault/slip data sets. *J. Struct. Geol.*, **v. 26**, pp. 919-925.
- Shan, Y.; Lin, G.; Li, Z. and Zhao, C. (2006). Influence of measurement errors on stress estimated from single-phase fault/slip data. *J. Struct. Geol.*, **v. 28**, pp. 943-951.
- Stern, R.J.( 1994). Arc-assembly and continental collision in the Neoproterozoic African orogen: implications for the consolidation of Gondwanaland. *Annual Review of Earth and Planetary Sciences*, **22**, 319–351.
- Stern, R. J., Gottfried, D., and Hedge, C. E. (1984). Late Precambrian rifting and crustal evolution in the Northeastern Desert of Egypt. *Geology* **12**: 168-172.
- Shan, Y., Fry, N., Lisle. R.L., 2009: Graphical construction for the direction of shear. *J. Struct. Geol.*, **Vol.31**, pp. 476- 478.
- Waheeb, A. G. and El Sundoly, H. I. (2020). Tensile stress and related Th-U-REE mineralizations in the granite of Wadi Ras Abda, North Eastern Desert, Egypt. . *Arabian Journal of Geosciences*. <https://doi.org/10.1007/s12517-020-05543-z>.
- Zalohar, J. and Vrabec, M. ( 2007). Paleostress analysis of heterogeneous fault-slip data: The Gauss Method, *J. Struct. Geol.*, **v. 29**, pp. 1798-1810.



Zhao, K., Jiang, S., Dong, C., Chen, W., Chen, P., Ling, H., Zhang, J., Kai-Xing Wang, K. (2011). Uranium-bearing and barren granites from the Taoshan Complex, Jiangxi Province, South China:

Geochemical and petrogenetic discrimination and exploration significance. *Journal of Geochemical Exploration* **110**:126–135.

مقارنة بين تمعدنات الثوريوم واليورانيوم والعناصر الأرضية النادرة في صخور الريوليت البركانية ومكافئها الجوفي: دراسة حاله للتمعدنات ذات الصلة بالتراكيب الجيولوجية المتواجدة بمنطقتي أم صافي ورأس عابدة، الصحراء الشرقية، مصر  
أنطون جورج وهيب، وحسن إسماعيل أحمد، ومحمد متولي حسن، وهشام محمود عبدالحמיד، وصديق حمدي صديق  
هيئة المواد النووية، القاهرة، جمهورية مصر العربية

تعتبر صخور الريوليت البركانية بمنطقه أم صافي واحدة من أكثر الصخور الملائمة لتواجد معادن العناصر الأرضية النادرة في وسط الصحراء الشرقية في مصر، والتي يُعتقد أنها مصدر عالي لمعادن العناصر الأرضية النادرة مصحوبا في الغالب بتواجد الثوريوم المشع. كما يُعتبر الجرانيت البيرثيتي القلوي عالي البوتاسيوم بمنطقه رأس عبدة مصدرًا عاليًا للمعادن المشعة في شمال الصحراء الشرقية في مصر. إن وجود تمعدنات العناصر الأرضية النادرة و الثوريوم و اليورانيوم في كل من الصخور البركانية الريوليتية بمنطقه أم صافي وفي الصخور الجرانيتية الجوفيه بمنطقه رأس عبدة مرتبط بحدوث حركات تكتونية داخلية بتلك المناطق وترتبط بنفس مرحلة التشوه في المنطقتين وهي مرحلة الشد في اتجاه WNW-ESE إلى E-W. النشاط الإشعاعي في منطقة أم صافي أعلى من منطقته رأس عبدة ولكن منطقة رأس عبدة أغنى بمعادن اليورانيوم من منطقة أم صافي. تم الكشف عن اليورانوفان واليورانونثوريت والثوريت في منطقة وادي رأس عبدة، بينما تم تحديد الثوريت في منطقة أم صافي. يشير التحليل التركيبي لإجهاد القص إلى أن اتجاه إجهاد القص ( $\tau$ ) في البراكين الريوليتية في منطقته أم صافي هو اتجاه شمال-جنوب، حيث ينحرف قليلاً إلى شمال شمال شرق-جنوب غرب وشمال شرق-جنوب غرب في مناطق الصدوع الجرانيتية المتمعدنة بمنطقه رأس عبدة.